Effects of Carbon Fillers on Tensile and Flexural Properties in Polypropylene-Based Resins

Daniel López Gaxiola, Mary M. Jubinski, Jason M. Keith, Julia A. King, Ibrahim Miskioglu

Department of Chemical Engineering, Michigan Technological University, Houghton, Michigan 49931-1295

Received 24 July 2009; accepted 1 April 2010
DOI 10.1002/app.32540
Published online 3 June 2010 in Wiley InterScience (www.interscience.wiley.com).

ABSTRACT: A potential application for conductive resins is in bipolar plates for use in fuel cells. The addition of carbon filler can increase the electrical and thermal conductivities of the polymer matrix but will also have an effect on the tensile and flexural properties, important for bipolar plates. In this research, three different types of carbon (carbon black, synthetic graphite, and carbon nanotubes) were added to polypropylene and the effects of these single fillers on the flexural and tensile properties were measured. All three carbon fillers caused an increase in the tensile and flexural modulus of the composite. The ultimate tensile and flexural strengths decreased with the addition of carbon black and synthetic graphite, but increased for carbon nanotubes/polypropylene composites due to the difference in the aspect ratio of this filler compared to carbon black and synthetic graphite. Finally, it was found that the Nielsen model gave the best prediction of the tensile modulus for the polypropylene based composites. © 2010 Wiley Periodicals, Inc. J Appl Polym Sci 118: 1620–1633, 2010

Key words: composites; fillers; polypropylene; mechanical properties; modeling

INTRODUCTION

Most polymer resins are insulating materials but they can also be used for other applications if their properties, such as electrical and thermal conductivity, are modified. One emerging market for conductive resins is bipolar plates for use in fuel cells. The bipolar plate has different functions. It separates one cell from the next, carrying hydrogen gas on one side and oxygen on the other side. Bipolar plates must be made of a material with low gas permeability, good dimensional stability and moderate flexural and tensile properties and with high thermal and electrical conductivity to conduct heat out of the cell and to minimize ohmic losses. The target set by the Department of Energy for flexural strength of bipolar plates is 25 MPa.[1] Plug Power (Latham, NY) has set a desired flexural strength of greater than 59 MPa and a desired tensile strength of greater than 41 MPa.[2]

One approach to improving conductivity of a polymer is the addition of a conductive filler material, such as carbon or metal.[3–9] Currently, a single type of graphite powder (often 60 wt %) is typically used in thermosetting resins (often a vinyl ester) to produce a thermally and electrically conductive bipolar plate material.[10–13] Thermosetting resins cannot be remelted.

Significant progress is being made to develop new recyclable materials with good mechanical properties for application in fuel cell bipolar plates.[9,14–29] Kalaitzidou et al.[26] and Akinci[28] added concentrations up to 50 wt % of graphite to a polypropylene matrix observed an increase in the tensile and flexural modulus of the composite. Other research groups[19,20,22,23,27,29] have measured the mechanical properties of composites containing carbon nanotubes concentrations up to 6 wt % in different polymer matrices. Their results have shown an improvement in both the tensile modulus and the ultimate tensile strength of the materials produced. A summary of tensile and flexural strength tests using carbon black, carbon nanotubes, and synthetic graphite is shown in Table I later.[9,14–18,21,22,24–26,28,29] In general, this table shows relatively consistent results for the fillers used. We noted that in this table, the work of Chodak et al.[18] compares composites made by injection molding (+ symbol) and compression molding (++ symbol). Better results were obtained with injection molding. Furthermore, Mali[24] investigated strength properties using acetylene carbon black and Vulcan carbon black and found similar results with both fillers.

With regard to utility in bipolar plates, Blunk et al.[30] prepared two formulations with polypropylene as the matrix. For a filler concentration of 15 wt % graphite fiber, 5 wt % carbon black, and 30 wt % carbon fiber, they obtained a flexural strength of 83 MPa and a flexural modulus of 16.9 GPa. For

Correspondence to: J. M. Keith (jmkeith@mtu.edu).
Contract grant sponsor: Department of Energy; contract grant number: DE-FG36-08GO88104.

TABLE I
Summary of Tensile and Flexural Test Results for Polypropylene Filled Composites

Authors	Filler (wt %)	Tensile strength (MPa)	Tensile modulus (GPa)	Flexural strength (MPa)	Flexural modulus (GPa)
Petrovic et al.[14]	N/A	29			1.2
Petrovic et al.[14]	CB (15)	28			2.0
Petrovic et al.[14]	CB (25)	26			2.7
Kaynak et al.[15]	N/A	29	1.0		
Kaynak et al.[15]	CB (15)	25	1.5		
Kaynak et al.[15]	CB (40)	35	3.2		
Chiu and Chiu[16]	N/A	31		34	1.3
Chiu and Chiu[16]	CB (13)	33		32	4.4
Chiu and Chiu[16]	CB (31)	28		44	7.4
Narkis et al.[17]	CB (15)	22			1.2
Chodak et al.[18]	N/A^{+}	41	0.8		
Chodak et al.[18]	N/A^{++}	36	0.8		
Chodak et al.[18]	CB^{+} (10)	36	1.2		
Chodak et al.[18]	CB^{++} (10)	31	1.0		
Arai et al.[21]	SG (85)			49	11.4
López Manchado et al.[22]	N/A	31	0.9		
López Manchado et al.[22]	SWCNT (0.75)	35	1.2		
López Manchado et al.[22]	CB (0.75)	33	0.9		
Mali[24]	N/A	21	0.5	32	0.9
Mali[24]	CB[a] (16)	20	0.9	31	0.8
Mali[24]	CB[a] (20)	20	0.9	30	0.9
Mali[24]	CB[a] (35)	13	0.4	33	1.0
Mali[24]	CB[b] (16)	20	0.9	31	0.8
Mali[24]	CB[b] (32)	11	0.6	31	0.9
Zhou et al.[25]	N/A	36			
Zhou et al.[25]	MWCNT (12.5)	37			
Zhou et al.[25]	CB (12.5)	37			
Kalaitzidou et al.[26]	N/A		1.5		1.3
Kalaitzidou et al.[26]	CB (6)		3.0		2.1
Bao and Tjong[9]	N/A	31	1.6		
Bao and Tjong[9]	MWCNT (1)	36	2.1		
Akinci[28]	SG (10)	29	2.5		
Akinci[28]	SG (30)	21	4.9		
Akinci[28]	SG (50)	17	5.5		
Ansari[29]	N/A	31	1.2		1.6
Ansari[29]	MWCNT (0.5)	34	1.5		1.6

Symbols:
$^{+}$ for injection molding, $^{++}$ for compression molding.
[a] for acetylene carbon black.
[b] for Vulcan carbon black.

comparison purposes, a composite with 40 wt % carbon fiber as a single filler led to a flexural strength of 28.9 MPa and a flexural modulus of 10.1 GPa. Mighri et al.[31] measured a flexural strength of 45 MPa and a flexural modulus of 8.0 GPa for polypropylene with 16.5 wt % carbon black and 38.5 wt % graphite. They also measured flexural strength of 52 MPa and a flexural modulus of 10.0 GPa for polypropylene with 16.5 wt % carbon black, 33.5 wt % graphite, and 5 wt % carbon fiber. When using a poly(phenylene sulfide) matrix, they obtained a flexural strength of 84 MPa and a flexural modulus of 19.0 GPa with 8.5 wt % carbon black, 43.8 wt % graphite, and 4 wt % carbon fiber. More recently, Cunnhingham et al.[32] proposed the production of wet-lay composite materials containing graphite in poly(ethylene terephthalate) and poly(phenylene sulfide). They obtained a tensile strength of up to 34 MPa and a flexural strength of up to 54 MPa.

As part of a larger project, research work in our laboratory has proposed the addition of higher concentrations of carbon fillers to a liquid crystal polymer (LCP) matrix[33–36] and a polypropylene matrix[37,38] to achieve a large enhancement of the thermal and electrical properties of the materials produced while maintaining good strength properties. As such, the focus of this article will be on the tensile and flexural properties and tensile modulus modeling of injection molded carbon/polypropylene composites. Polypropylene is a thermoplastic that can be remelted and used again. Three different carbon fillers (electrically conductive carbon black,

TABLE II
Properties of Dow's H7012-35RN Polypropylene Resin[39]

Melting point	163°C
Glass transition temperature	−6.6°C
Melt flow rate (230°C/2.16 kg)	35 g/10 min
Density	0.9 g/cc

synthetic graphite particles and carbon nanotubes) were studied. Composites containing various amounts of a single type of carbon filler were fabricated and tested. The goal of this work was to determine the effects of these fillers on the composite tensile and flexural properties. Properties of these composites were compared to results from prior work for carbon/LCP matrix composites.

EXPERIMENTAL

Materials

The matrix used for this project was Dow's semicrystalline homopolymer polypropylene resin H7012-35RN (Midland, MI). The properties of this polymer are shown in Table II.[39] The flexural and tensile results for polypropylene composites will be compared with those in a Ticona Vectra A950RX liquid-crystal polymer matrix (Summit, NJ). Vectra is a highly ordered thermoplastic copolymer consisting of 73 mol % hydroxybenzoic acid and 27 mol % hydroxynaphtoic acid. Properties of Vectra are shown elsewhere.[35]

The first filler used in this study was Ketjenblack EC-600 JD. This is an electrically conductive carbon black available from Akzo Nobel (Chicago, IL). The highly branched, high surface area carbon black structure allows it to contact a large amount of polymer, which results in improved electrical conductivity at low carbon black concentrations (often 5–7 wt %). The properties of Ketjenblack EC-600 JD are given in Table III.[40] The carbon black is in the form of pellets that are 100 μm to 2 mm in size and, upon mixing into a polymer, easily separate into primary aggregates 30–100 nm long.[40] A diagram of this carbon black structure is shown in Figure 1.

Table IV shows the properties of Asbury Carbons' Thermocarb TC-300 (Asbury, NJ), which is a primary synthetic graphite that was previously sold by Conoco.[41,42] Thermocarb TC-300 is produced from a thermally treated highly aromatic petroleum feedstock and contains very few impurities. A photomicrograph of this synthetic graphite is shown in Figure 2.

TABLE III
Properties of Akzo Nobel Ketjenblack EC-600 JD[40]

Electrical resistivity	0.01–0.1 Ω cm
Aggregate size	30–100 nm
Specific gravity	1.8 g/cm^3
Apparent bulk density	100–120 kg/m^3
Ash content, max	0.1 wt %
Moisture, max.	0.5 wt %
Brunauer–Emmett–Teller surface area	1250 m^2/g
Pore volume	480–510 cm^3/100 g

Figure 1 Structure of Ketjenblack EC − 600 JD.

Hyperion Catalysis International's FIBRIL™ nanotubes (Cambridge, MA) were the third filler used in this study. This is a conductive, vapor grown, multiwalled carbon nanotube. They are produced from a high purity, low molecular weight hydrocarbon in a proprietary, continuous, gas phase, catalyzed reaction. The outside diameter of the nanotube is 10 nm and the length is 10 μm, which gives an aspect ratio (length/diameter) of 1000. Due to this high aspect ratio, very low concentrations of nanotubes are

TABLE IV
Properties of Thermocarb TC-300 Synthetic Graphite[41,42]

Filler	Thermocarb TC-300 synthetic graphite
Carbon content (wt %)	99.91
Ash (wt %)	<0.1
Sulfur (wt %)	0.004
Density (g/cc)	2.24
Brunauer–Emmett–Teller surface area (m^2/g)	1.4
Thermal conductivity at 23°C (W/m K)	600. in "a" crystallographic direction
Electrical resistivity of bulk carbon powder at 150 psi, 23°C, parallel to pressing axis (Ω cm)	0.020
Particle shape	Acircular
Particle aspect ratio	1.7
Sieve analysis (wt %)	
+600 μm	0.19
+500 μm	0.36
+300 μm	5.24
+212 μm	12.04
+180 μm	8.25
+150 μm	12.44
+75 μm	34.89
+44 μm	16.17
−44 μm	10.42

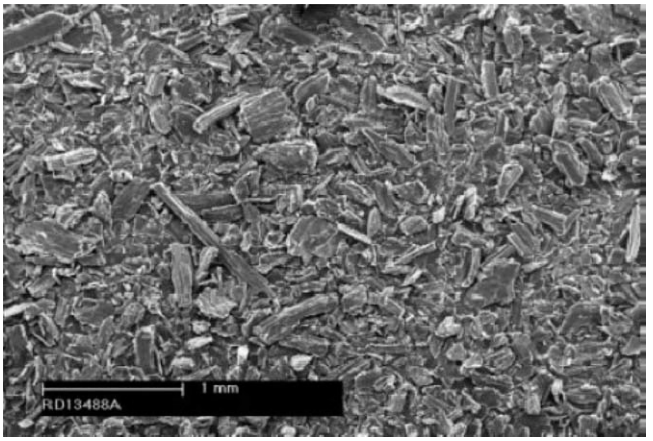

Figure 2 Photomicrograph of Thermocarb TC-300 synthetic graphite. (Courtesy of Asbury Carbons).

needed to produce an electrically conductive composite. This material was provided by Hyperion Catalysis International in a 20 wt % FIBRIL™ masterbatch MB3020-01. Table V shows the properties of this carbon filler.[43]

The concentrations (shown in wt % and the corresponding vol %) for all of the single filler composites in polypropylene tested in this research are shown in Table VI. In this and following tables and text, the abbreviation "PP" is used to signify polypropylene, "CB" is used to signify carbon black (Ketjenblack EC-600JD), "SG" is used for synthetic graphite (Thermocarb TC-300), and "CNT" is used for carbon nanotube (FIBRIL™). We note that increasing filler amount increases composite melt viscosity. Due to the large increase in composite melt viscosity, carbon black is only used at low loading levels.[44] The maximum single filler content that could be extruded and injection molded into test specimens were 15 wt % for carbon black, 80 wt % for synthetic graphite, and 15 wt % for carbon nanotubes.

It is noted that our studies cover a wider range in the amount of filler used (formulations ranged from six to fifteen different filler loadings), types of filler (three fillers were used), and types of matrix materials (in a later section we will compare results for polypropylene composites with Vectra LCP composites) when compared with the scientific literature summary of Table I.[9,14–18,21,22,24–26,28,29] This not only aids in interpretation of experimental results for fuel cell bipolar plate applications, but also allows for a tensile module modeling study which will be described later.

TABLE V
Properties of FIBRIL™ Carbon Nanotubes[43]

Composition	Pure carbon with trace residual metal oxide catalyst
Diameter	0.01 μm
Length	10 μm
Morphology	Typically eight graphitic sheets wrapped around a hollow 0.005 μm core
Brunauer–Emmett–Teller (N_2) surface area	250 m^2/g
Density	2.0 g/cc

TABLE VI
Single Filler Loading Levels in Polypropylene

Filler (wt %)	Ketjenblack (vol %)	Thermocarb (vol %)	Carbon nanotubes (vol %)
2.5	1.27	N/A	1.14
4.0	2.04	N/A	1.84
5.0	2.56	N/A	2.31
6.0	3.09	N/A	2.79
7.5	3.90	N/A	3.52
10.0	5.26	4.27	N/A
15.0	8.11	6.62	7.36
20.0	N/A	9.13	N/A
25.0	N/A	11.81	N/A
30.0	N/A	14.69	N/A
35.0	N/A	17.79	N/A
40.0	N/A	21.13	N/A
45.0	N/A	24.74	N/A
50.0	N/A	28.66	N/A
55.0	N/A	32.93	N/A
60.0	N/A	37.60	N/A
65.0	N/A	42.70	N/A
70.0	N/A	48.40	N/A
75.0	N/A	54.66	N/A
80.0	N/A	61.64	N/A

Test specimen fabrication

For this entire project, the fillers and polypropylene were used as- received. The extruder used was an American Leistritz Extruder Corporation Model ZSE 27 (Somerville, NJ). This extruder has a 27 mm corotating intermeshing twin screw with 10 zones and a length/diameter ratio of 40. The screw design, which is shown elsewhere,[44] was chosen to obtain a minimum amount of filler degradation, while still dispersing the fillers well in the polymers. The pure polypropylene pellets and the Hyperion FIBRIL™ masterbatch MB3020-01 (containing 20 wt % carbon nanotubes) were introduced in Zone 1. Synthetic graphite and carbon black were added into the polymer melt at Zone 5. Schenck AccuRate (Whitewater, WI) gravimetric feeders were used to accurately control the amount of each material added to the extruder. A typical temperature profile for extrusion is shown in Table VII.

After passing through the extruder, the polymer strands (3 mm in diameter) entered a water bath and then a pelletizer that produced nominally 3 mm long pellets. After extrusion, polypropylene based composites were dried in an indirect heated

dehumidifying drying oven at 80°C for 4 h and then stored in moisture barrier bags before injection molding.

A Niigata (Tokyo, Japan) injection molding machine, model NE85UA$_4$, was used to produce test specimens. This machine has a 40 mm diameter single screw with a length/diameter ratio of 18. The lengths of the feed, compression, and metering sections of the single screw are 396 mm, 180 mm, and 144 mm respectively. A typical injection molding temperature profile was 149°C (zone 1, feed), 204°C (zone 2), 216°C (zone 3), and 227°C (zone 4, nozzle). A four cavity mold was used to produce 3.3 mm thick ASTM Type I tensile bars (end-gated) and 3 mm thick, 127 mm long, 12.3 mm wide flexural bars (end-gated).

Synthetic graphite length, aspect ratio, and orientation test method

To determine the length and aspect ratio (length/diameter) of the synthetic graphite in the composites, xylene at 120°C was used to dissolve the polypropylene matrix. The fillers were then dispersed onto a glass slide and viewed using an Olympus SZH10 optical microscope with an Optronics Engineering LX-750 video camera (Orangeburg, NY). The filler images (at 70× magnification) were collected using Scion Image Version 1.62 software. The images were then processed using Adobe Photoshop 5.0 (San Jose, CA) and the Image Processing Tool Kit version 3.0 (Natick, MA). The length and aspect ratio of each particle was measured. For each formulation, ~ 1,000 particles were measured. To determine the orientation of the synthetic graphite in the tensile and flexural specimens, the samples were cast in epoxy so that the direction of flow induced during the injection-molding process, which was also the lengthwise direction, would be viewed. The samples were then polished and viewed with an Olympus BX60 reflected light microscope at a magnification of 200×. Adobe Photoshop 5.0 and the Image Processing Tool Kit version 3.0 were used to process the images. For each formulation, the orientation was determined by viewing typically 1000 particles.

Tensile test method

The tensile properties (at ambient conditions, 165 mm long, 3.3 mm thick ASTM Type I sample geometry) from all formulations were determined with ASTM D 638 at a crosshead rate of 5 mm/min for reinforced plastics.[45] An Instru-Met Sintech screw-driven mechanical testing machine was used. The tensile modulus was calculated from the initial linear portion of the stress–strain curve. For each formulation, at least five samples were tested.

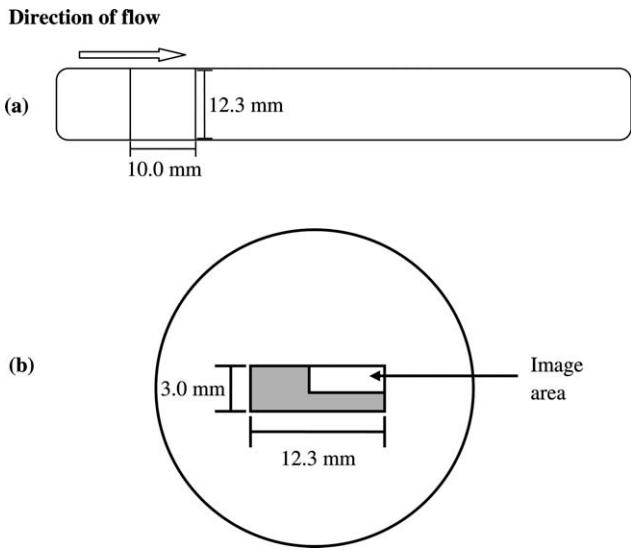

Figure 3 (a) Portion of flexural bar from where nanoscratch specimens were cut. (b) Sample arrangement for nanoscratch testing.

Flexural test method

The flexural properties were determined with three-point loading under ambient conditions from all formulations, according to ASTM D 790 at a crosshead rate of 5.3 mm/min.[46] Each rectangular sample was 3 mm thick, 127 mm long and 12.3 mm wide. A span of 48 mm (corresponding to a 16 : 1 span/thickness ratio) was used in an Instru-Met (Union, NJ) Sintech screw-driven mechanical testing machine. Deflection was measured with a linear variable displacement transducer. The flexural modulus was calculated from the initial linear portion of the load- deflection curve. For each formulation, at least five samples were tested.

Nanoscratch testing

Nanoscratch tests were performed on samples cut from the center of flexural specimens for the formulation containing 20 wt % of Thermocarb TC-300 in polypropylene, as shown in Figure 3(a). Then, the 3 mm thick × 12.3 mm long face was mounted in epoxy, as shown in Figure 3(b), and tested with a MTS Nano Indenter XP (Oak Ridge, TN). The typical test was run under a constant load of 40 mN. The scratch length was 500 μm, the scratch speed was 10 μm/s, and data were sampled at 5 Hz.

For each sample, two batches of five scratches were made and two test samples were used for the composite and one sample for the neat polypropylene. A Berkovich indenter was used for the tests with scratches made in the edge-forward direction, as shown in Figure 4. Data collected included force on sample, penetration of the indenter relative to the surface of the sample, force along the scratch

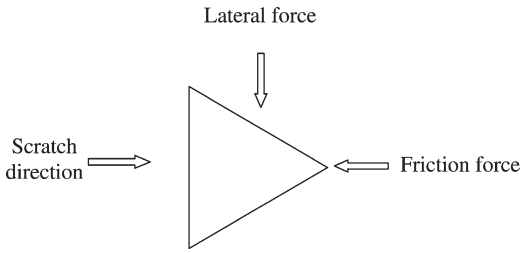

Figure 4 Scratch direction used in the tests with the Berkovich indenter.

direction (friction force), and force normal to the scratch direction (lateral force). All the data were recorded with respect to distance along the scratch. The friction and lateral forces are also depicted in Figure 4.

A scratch test is performed in three stages, the original profile, the scratch segment, and the residual profile. The original profile is obtained under a very small load (20 μN) and is used to determine the original morphology of the surface along the scratch path. This information is then used to correct the depth measurements during the scratch segment for roughness and initial slope of the sample. The same corrections are applied in the determination of the residual profile. In this study, the information on the residual profile was not used in the analysis.

The penetration during scratch was characterized by the crest factor,[47] a parameter used as a measure of spikeness in the data. This measure is mainly used in digital signal analysis of waveforms and is defined as the peak amplitude divided by the root mean square of the penetration:

$$\text{Crest factor} = \frac{|y_{max} - y_{min}|}{2\sqrt{\frac{1}{N}\sum_{j=0}^{N-1} y_j^2}} \quad (1)$$

where y_{max} is the maximum penetration along the scratch length, y_{min} is the minimum penetration along the scratch length, y is the penetration (nm) along the scratch length and N is the number of data points considered for a given scratch. During a typical scratch test, data is collected over 500 μm. To avoid any end effects at the beginning and end of the scratch length, data over the first and last 10 μm of the scratch were omitted in the calculations of the crest factor.

Scratch tests performed on a heterogeneous material under a constant normal load give the local compliance of the material, so it is possible to detect the filler-rich and matrix-rich areas along the scratch path. A shallow scratch depth indicates a high-stiffness (filler-rich) area, and a larger scratch depth indicates a lower stiffness (matrix-rich) area. Because the width of the groove generated by the scratch tip (ca. 30 μm) is large compared to the small size of the carbon black and carbon nanotubes, these composites could not be studied using the nanoscratch method. This method was only used in the composites containing synthetic graphite.

RESULTS AND DISCUSSION

Filler Length, aspect ratio and orientation results

The injection molded polypropylene test specimens filled with Thermocarb TC-300 had a filler aspect ratio of 1.67 and a length of 40 μm. Because the tensile and flexural test specimens are end-gated, the synthetic graphite is primarily aligned with the length of the tensile specimens. These results show good agreement with values obtained from prior work for nylon, polycarbonate and LCP resins.[48–50] Photomicrographs showing the orientation of the synthetic graphite are shown elsewhere.[36,44,48,49,51] Photomicrographs showing the dispersion of carbon nanotubes and carbon black are shown elsewhere.[38] We note that the aspect ratio and length of the carbon black could not be measured due to the small size of the particles (30–100 nm). Carbon nanotubes had a length of 10 μm and a diameter of 0.01 μm. These values provided by the vendor yielded an aspect ratio of 1000 for this filler.[43]

Tensile test results

Figure 5 shows typical stress–strain graphs for the composite materials used in this study. The tensile modulus, ultimate tensile strength, and strain at ultimate tensile strength results are shown in Figures 6–8 for carbon/polypropylene composites, as the mean

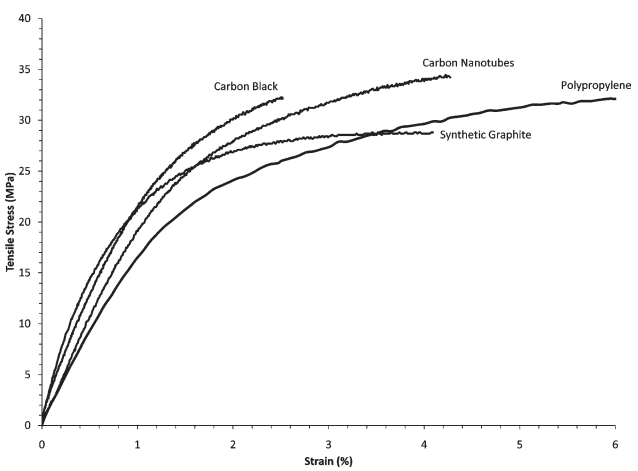

Figure 5 Typical tensile stress–strain plots for pure polypropylene (initial portion), polypropylene with 6 wt % carbon black, polypropylene with 20 wt % synthetic graphite, and polypropylene with 6 wt % carbon nanotubes.

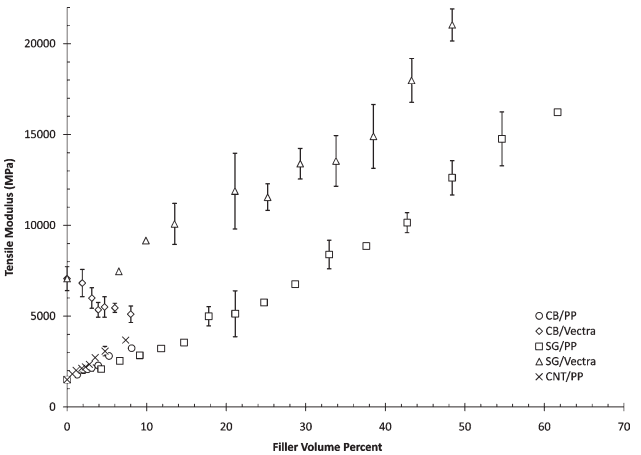

Figure 6 Single filler tensile modulus results for CB/PP, SG/PP, CNT/PP, CB/vectra, and SG/vectra composites.

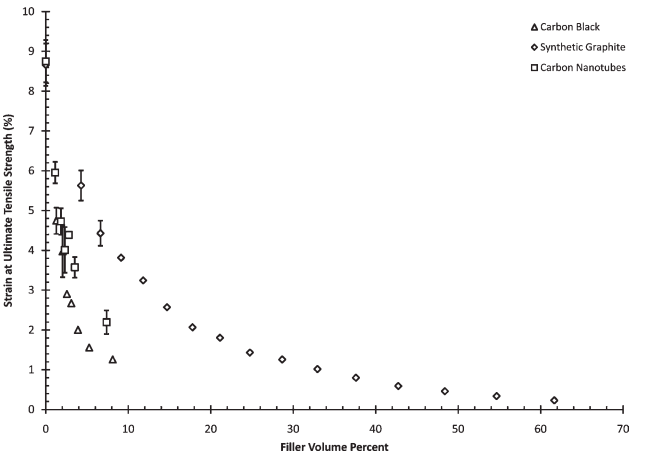

Figure 8 Strain at ultimate tensile strength for polypropylene composites containing various amounts of single fillers.

plus or minus one standard deviation, as a function of the filler volume fraction. The error bars are not shown for formulations where one standard deviation is less than the marker size. It is noted that results for Vectra composites are also included in Figures 6 and 7. These results will be discussed in the next section. For all the carbon/polypropylene samples tested, the ultimate tensile strength values were the same as the fracture tensile strength.

Figure 6 shows the tensile modulus as a function of the filler volume fraction, for formulations containing single fillers in polypropylene. The measured value of the tensile modulus of pure PP was 1510 MPa. In Figure 6 it can be seen that higher concentrations of all carbon fillers in the polypropylene matrix caused an increase in the tensile modulus of the composite. This can be explained by the fact that the tensile modulus of the fillers is much higher than that of the neat polypropylene.[49,52–54] The adhesion between the filler and the matrix may also contribute to this effect, and will be described in a following subsection. Based upon a comparison at low filler concentrations, the largest relative increase was observed in formulations containing carbon nanotubes, followed by formulations containing carbon black. We also note that the largest value of the tensile modulus measured in our experiments was 16,200 MPa at a concentration of 61.64 vol % (80 wt %) synthetic graphite. These results compare well with those in the literature, which shows an increase in tensile modulus as the fillers used in this study are added to polypropylene.[9,15,18,22,24,26,28,29]

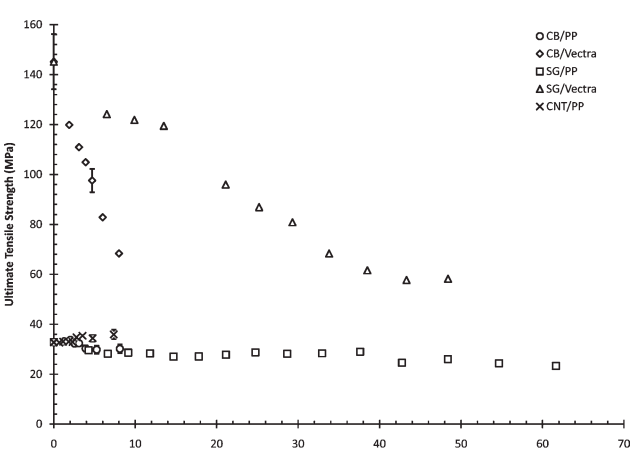

Figure 7 Single filler ultimate tensile strength results for CB/PP, SG/PP, CNT/PP, CB/vectra, and SG/vectra composites.

Figure 7 shows the ultimate tensile strength for composites containing various amounts of single filler in polypropylene. In general, the ultimate tensile strength is relatively unchanged for all systems studied. It can be seen that carbon black causes a decrease in the ultimate tensile strength, which agrees with those seen in the literature at low filler loadings.[14,15,18,24] The results of Chiu and Chiu[16] and Zhou et al.[25] show a very slight increase in ultimate tensile strength. Composites containing synthetic graphite particles had a similar decrease to carbon black in the values of the ultimate tensile strength. The behavior of the ultimate tensile strength using synthetic graphite agrees with prior work by Konell et al.[49] and with Akinci[28] for synthetic graphite in polypropylene. This result is likely because synthetic graphite (with an aspect ratio of 1.67) is not a reinforcing material.

Also in Figure 7, opposite to what occurred with carbon black and synthetic graphite, it can be seen that the addition of carbon nanotubes caused the ultimate tensile strength to increase slightly, similar to that observed by others when low concentrations of carbon nanotubes are added to polypropylene.[9,22,29,55] This result is expected due to the high aspect ratio (1000) of the carbon nanotubes.[40]

TABLE VII
Temperature Profile for Extrusion

Extruder zone	Temperature (°C)
Feed zone	Water cooled
Heated zone 1	150
Heated zone 2	180
Heated zone 3	195
Heated zone 4	210
Heated zone 5	220
Heated zone 6	220
Heated zone 7	220
Heated zone 8	220
Heated zone 9	220
Heated zone 10 (Die End)	220

The strain at ultimate tensile stress results for the carbon black, synthetic graphite and carbon nanotubes in polypropylene are illustrated in Figure 8. As expected, it can be observed that strain values for all three fillers decrease when filler is added. At the highest concentrations of carbon fillers, the strain at ultimate strength values were reduced the most with carbon black, followed by carbon nanotubes. This decrease in the strain at ultimate tensile strength with the addition of carbon fillers, agrees with results observed by Huang[56] and Konell et al.[49] We also note that at the largest loading of synthetic graphite, 61.64 vol % (80 wt %), the strain at ultimate tensile strength was measured to be 0.23%.

Comparison of tensile results for polypropylene and liquid crystal polymer composites

Because prior tensile and flexural strength tests were performed using carbon black and synthetic graphite in a Vectra liquid crystal polymer matrix (LCP) for use in fuel cell bipolar plate applications,[35] a comparison is made in Figures 6 and 7. The filler volume fractions used in the LCP matrix are summarized in Table VIII.[35] The tensile modulus increased as a function of the filler volume percent with increasing filler concentration for both carbon black and synthetic graphite in the polypropylene, as indicated in Figure 6. This result is consistent for synthetic graphite in the LCP matrix. However, the addition of carbon black to LCP resulted in a reduction in tensile modulus, in contrast with the increase in tensile modulus seen in the carbon black/polypropylene composites. Prior work has shown that Vectra has had poor adhesion to some carbon fillers,[57,58] and we hypothesize that carbon black may also have poor adhesion to Vectra, which may explain the poor tensile modulus results in Vectra.

Figure 7 shows that both carbon black and synthetic graphite caused the ultimate tensile strength to decrease for LCP and polypropylene composites; however, the reduction is much more significant in the LCP composites. Carbon black in polypropylene caused the smallest decrease in the ultimate tensile strength with values of 32.7 MPa for the neat polymer and 30.2 MPa for a concentration of 8.11 vol % (15 wt %) of carbon black. For comparison, the ultimate tensile strength for neat Vectra was 145.2 MPa and decreased to 68.4 MPa with a carbon black loading of 7.95 vol % (10 wt %). This result supports our hypothesis that carbon black may have poor adhesion to Vectra. Finally, the composites formed with synthetic graphite and polypropylene has an ultimate tensile strength of 26.0 MPa at a concentration of 48.40 vol % (70 wt %), which can be compared to the synthetic graphite/Vectra composite at 58.2 MPa at 48.39 vol % (60 wt %).

Overall, the tensile modulus and ultimate tensile strength of the composites with Vectra as the polymer matrix were higher due to its liquid crystal structure. The rod-like shaped structure of the solid LCP contributes to the reinforcement of the composite.[59,60]

Flexural test results

Figures 9–11 show the flexural test results for each formulation. When the standard deviation for each formulation was less than the marker size in the graphs, the error bars were not displayed. Figures 9–10 also show the results for carbon/Vectra composites, which will be described in the next section. The flexural modulus results for composites with varying amounts of the single fillers in polypropylene are shown in Figure 9. For the pure polypropylene, the experimental flexural modulus is 1700 MPa. Adding each of the three single carbon fillers caused an increase in the flexural modulus. The largest effect is due to carbon nanotubes, followed by carbon black. As a final note, the maximum flexural

TABLE VIII
Single Filler Loading Levels in Vectra A950RX[35]

Filler (wt %)	Ketjenblack (vol %)	Thermocarb (vol %)
2.5	1.96	N/A
4.0	3.14	N/A
5.0	3.93	N/A
6.0	4.73	N/A
7.5	5.93	N/A
10.0	7.95	6.49
15.0	N/A	9.93
20.0	N/A	13.51
25.0	N/A	17.24
30.0	N/A	21.13
35.0	N/A	25.18
40.0	N/A	29.41
45.0	N/A	33.83
50.0	N/A	38.46
55.0	N/A	43.31
60.0	N/A	48.39

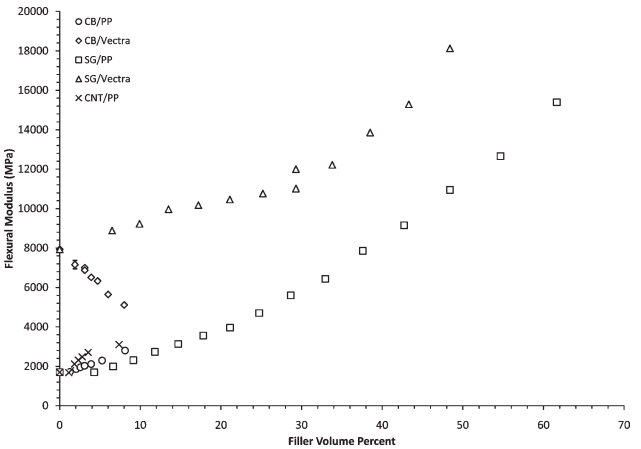

Figure 9 Single filler flexural modulus results for CB/PP, SG/PP, CNT/PP, CB/vectra, and SG/vectra composites.

modulus for our experiments was 15,400 MPa which was obtained with synthetic graphite at 61.64 vol % (80 wt %).

It can be seen that the flexural modulus behavior as function of the volume fraction of the fillers, followed the same trend observed in the tensile modulus results. The change in the properties of the pure polypropylene can be attributed to the higher modulus of the carbon fillers. If we compare the results of different fillers at low concentrations in Figure 9, it can be seen that the largest increase was observed in composites containing carbon nanotubes, due to the high aspect ratio of the filler. The carbon black[14,16,24,26] and synthetic graphite[21] results are consistent with that seen in the literature. Ansari[29] found no increase in flexural modulus with addition of 0.5 wt % multiwalled carbon nanotubes. However, both López Manchado et al.[22] and Ansari[29] found an increase in tensile modulus with increasing concentration of carbon nanotubes.

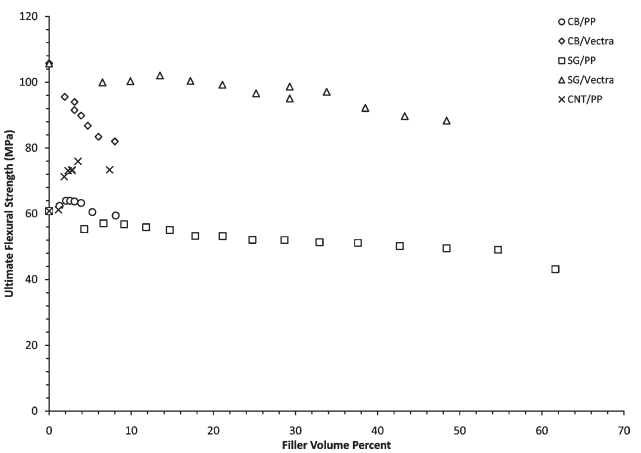

Figure 10 Single filler ultimate flexural strength results for CB/PP, SG/PP, CNT/PP, CB/vectra, and SG/vectra composites.

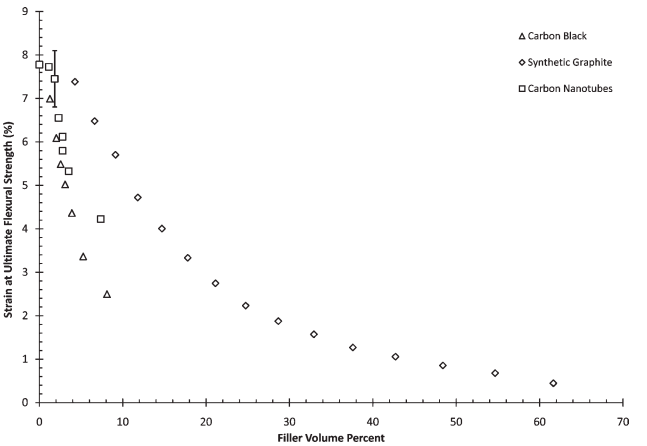

Figure 11 Strain at ultimate flexural strength for polypropylene composites containing various amounts of single fillers.

In Figure 10, it can be seen that the ultimate flexural strength of pure polypropylene was 60.8 MPa. For comparison purposes, the addition of carbon nanotubes caused an increase in the ultimate flexural strength to 73.4 MPa for composites with 7.36 vol % (15 wt %), due to the high aspect ratio of carbon nanotubes. The increase in flexural strength is consistent with the increase in tensile strength seen in our results (Fig. 7) and in the literature.[9,22,29,55] The addition of 8.11 vol % (15 wt %) carbon black led to a decrease in ultimate flexural strength to 59.5 MPa. This is consistent with that seen in the literature.[16,24] Finally, it is noted that at the highest concentration used for each of three fillers, the composites containing a concentration of 61.64 vol % (80 wt %) synthetic graphite had the lowest ultimate flexural strength (43.1 MPa).

Figure 11 illustrates the strain at ultimate flexural strength results for composites filled with carbon black, synthetic graphite and carbon nanotubes. As expected, the addition of any of these fillers caused the strain to decrease. In comparison, synthetic graphite led to the lowest decrease in strain, followed by carbon nanotubes. The lowest value was observed in composites with synthetic graphite, which was 0.44% for a filler concentration of 61.64 vol % (80 wt %) of synthetic graphite particles.

Comparison of flexural results for polypropylene and liquid crystal polymer composites

Figures 9–10 show the mean flexural modulus and ultimate flexural strength, respectively and one standard deviation for at least five specimens tested of composites with carbon black and synthetic graphite in polypropylene and in Vectra A950RX LCP matrices. Similar with the tensile results, synthetic graphite caused an increase in the flexural modulus in both matrices. In the polypropylene

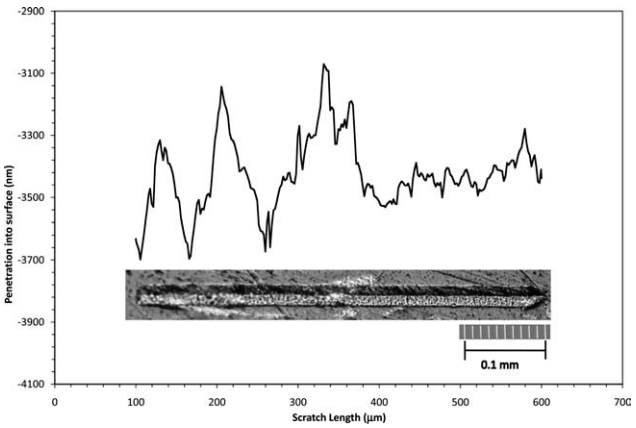

Figure 12 Displacement normal to the surface under a constant force of 40 mN for composites containing 20 wt % of synthetic graphite particles in polypropylene.

matrix, the addition of carbon black caused an increase in the flexural modulus from 1700 MPa for the pure polypropylene to 2800 MPa at a carbon black concentration of 8.11 vol % (15 wt %) carbon black. As described earlier, this may be due to poor adhesion between carbon black and Vectra.

As expected, a decrease in the ultimate flexural strength was observed in the composites with single amounts of carbon black and synthetic graphite in polypropylene and LCP as it can be seen in Figure 10. At a concentration of 8.11 vol % (15 wt %) of carbon black in polypropylene, the value measured for the ultimate flexural strength was 59.5 MPa and for the LCP composites with 7.95 vol % (10 wt %) carbon black, an ultimate flexural strength of 82.0 MPa was observed. The addition of synthetic graphite also caused a decrease in the ultimate flexural strength of the composites in the two different matrices. The ultimate flexural strength value measured for the composites containing 48.40 vol % (70 wt %) synthetic graphite in polypropylene was 49.5 MPa. The composites with 48.39 vol % (60 wt %) synthetic graphite in LCP, had an ultimate flexural strength of 88.3 MPa. Again, the carbon/Vectra composites have better flexural properties than the carbon/polypropylene composites due to the liquid-crystalline structure of the Vectra.

Nanoscratch results

The indenter displacement as a function of the scratch distance for the formulation containing 20 wt % of synthetic graphite in polypropylene is shown in Figure 12. The degree of adhesion between the synthetic graphite particles and the polypropylene matrix affected the transition regions in the plot, between the filler-rich area (lower penetration) and matrix-rich areas (higher penetration). A photomicrograph of the scratch surface is also shown in Figure 12.

Table IX shows the results for the crest factor, comparing the penetration of the indenter into composites containing 20 wt % in Vectra A950RX LCP and in the polypropylene matrix used in this project.[61] Previous research[62] has shown that the normalized crest factor (ratio of the composite crest factor to the polymer crest factor) can be used as a measure to compare the relative degree of adhesion between different composites having the same matrix but different types of fillers. A higher normalized crest factor is indicative of a resistance of the composite to scratching, due to better filler/matrix adhesion.

Table IX shows that the crest factor for the matrix materials polypropylene and Vectra were close to zero, because there was no filler causing perturbation in the displacement. Table IX also shows the normalized crest factor used to estimate the effect of filler/matrix adhesion. If we correlate the nanoscratch results to the ratio of composite tensile modulus to matrix tensile modulus, we find for 48.40 vol % (70 wt %) of synthetic graphite in polypropylene, a modulus enhancement ratio of 8.4 is found (12600 MPa/1510 MPa), while for 48.39 vol % (60 wt %) of synthetic graphite in Vectra, a modulus enhancement ratio was found to be 3.0 (21000 MPa/7070 MPa) which might be attributed to better filler/matrix adhesion for the polypropylene composites.

TENSILE MODULUS MODELING

Background

Many models[63] are used to predict the tensile modulus of a two-component composite material (for example, one matrix material and one filler). Shown below are the most basic models.

$$E_c = V_m E_m + V_f E_f \quad \text{Rule of mixtures (series model)} \tag{2}$$

TABLE IX
Penetration Crest Factors for Polymer Composites with 20 wt % Synthetic Graphite in Different Matrices[59]

Formulation	Number of scratch tests performed	Mean crest factor	Normalized crest factor (matrix = 1.00)
Thermocarb/ vectra	10	0.149	1.79
Thermocarb/ polypropylene	10	0.110	5.03
Pure vectra	10	0.083	1.00
Pure polypropylene	5	0.022	1.00

$$\frac{1}{E_c} = \frac{V_m}{E_m} + \frac{V_f}{E_f} \quad (3)$$

Inverse rule of mixtures (parallel model)

where: E_c = composite tensile modulus
V_f = volume fraction of filler
V_m = volume fraction of matrix = $1 - V_f$
E_m = tensile modulus of matrix
E_f = tensile modulus of filler

The rule of mixtures model typically overpredicts the modulus of short fiber/particulate composites, whereas the inverse rule of mixtures model typically underpredicts the modulus of short fiber/particulate composites.

More detailed models such as the Halpin-Tsai equations can be used to predict the modulus of short fiber composites.[63–66] The analysis uses the longitudinal and transverse moduli of aligned unidirectional (oriented) short fiber composites, given below.

$$\frac{E_L}{E_m} = \frac{1 + 2(L/d)\eta_L V_f}{1 - \eta_L V_f} \quad (4)$$

$$\frac{E_T}{E_m} = \frac{1 + 2\eta_T V_f}{1 - \eta_T V_f} \quad (5)$$

$$\eta_L = \frac{(E_f/E_m) - 1}{(E_f/E_m) + 2(L/d)} \quad (6)$$

$$\eta_T = \frac{(E_f/E_m) - 1}{(E_f/E_m) + 2} \quad (7)$$

where: E_L = longitudinal composite tensile modulus
E_T = transverse composite tensile modulus
L = filler length
d = filler diameter

It is noted that eq. (4) will be referred to in this article as the Halpin-Tsai oriented fiber model.

The longitudinal and transverse models can be combined for a two-dimensional random orientation of fibers, as shown in eq. (8),[63] and for a three-dimensional random orientation of fibers, as shown in eq. (9).[64]

$$E_c = \frac{3}{8}E_L + \frac{5}{8}E_T \quad \text{2D Randomly oriented fiber} \quad (8)$$

$$E_c = \frac{1}{5}E_L + \frac{4}{5}E_T \quad \text{3D Randomly oriented fiber} \quad (9)$$

Nielsen[67–70] has developed a macroscopic model that is the most versatile for short fiber/particulate composites. It accounts for constituent properties and concentrations of each constituent. Furthermore, the aspect ratio, orientation, and packing of the fillers in included in the model

$$\frac{E_c}{E_m} = \frac{1 + \mathrm{ABV_f}}{1 - B\psi V_f} \quad (10)$$

$$A = k_E - 1 \quad (11)$$

$$B = \frac{E_f/E_m - 1}{E_f/E_m + A} \quad (12)$$

$$\psi \cong 1 + \frac{1 - \phi_m}{\phi_m^2}\mathrm{V_f} \quad (13)$$

where ϕ_m = maximum packing fraction of the filler.

The constant A in eq. (11) is related to the generalized Einstein coefficient, which is a function of the aspect ratio and orientation (random vs. unidirectional) of the filler, while ϕ_m is based on the particle shape (sphere, irregular particles, fibers) and packing order (random loose, random close, three-dimensional random, etc). In eq. (12), the relative modulus of the two components (one matrix and one filler) is captured in the parameter B. In eq. (13), the factor Ψ is related to the maximum packing fraction of the filler. We note that the value of ΦV_f, equivalent to a reduced volume fraction, approaches 1.0 when $V_f = \phi_m$.

Alternatives to eq. (13) have also been proposed by McGee and McCullough[69,71]:

$$\psi \cong 1 + \frac{V_m}{\phi_m}\left[\phi_m V_f + (1 - \phi_m)V_m\right] \quad (14)$$

In this work, eqs. (10)–(12) and (14) are referred as the Modified Nielsen model.

Modeling results

All the above tensile modulus models use the tensile modulus of each constituent. Based on the previous experimental results, the tensile modulus of polypropylene was 1500 MPa. In previous modeling research on nylon 6,6 and polycarbonate composites,[52] the modulus of Thermocarb TC-300 used was 827 GPa and the modulus of Ketjenblack EC-600 JD was 827 GPa. The modulus of carbon nanotubes is available in the recent literature[53,54,72,73] and in the range of 900–1060 GPa. As such, we use 1000 GPa for our modeling work.

In addition to filler tensile modulus, some of the models need the filler aspect ratio (L/d). For synthetic graphite, the aspect ratio used was 1.67. For carbon nanotubes, the aspect ratio used was 1000.[43] Finally, it is assumed that carbon black is a spherical particle. As such, a value of 1.5 was used instead of

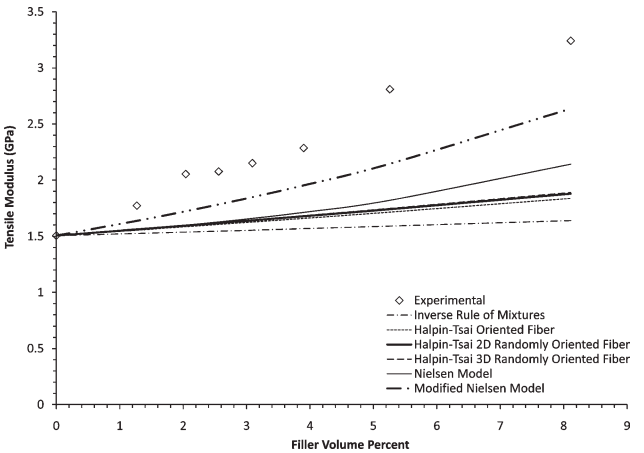

Figure 13 Tensile modulus modeling for carbon black in polypropylene. From lowest to highest, the models are Inverse Rule of Mixtures, Halpin-Tsai Oriented Fiber, 2D Halpin-Tsai, 3D Halpin-Tsai, Nielsen, and Modified Nielsen.

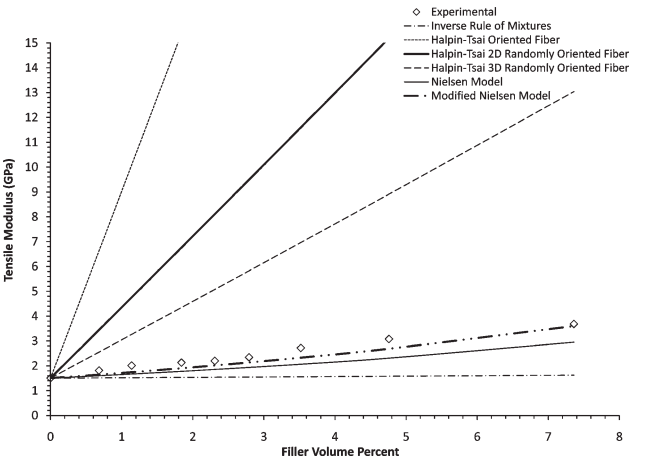

Figure 15 Tensile modulus modeling for carbon nanotubes in polypropylene. From lowest to highest, the models at are Inverse Rule of Mixtures, Nielsen, Modified Nielsen, 3D Halpin-Tsai, 2D Halpin-Tsai, and Halpin-Tsai Oriented Fiber.

$2(L/d)$ in the Halpin-Tsai model.[67,68] We note that due to the particle shape, all of the Halpin-Tsai equations become the same for carbon black composites.

Basic and Halpin-Tsai models

Tensile modulus values predicted by the inverse rule of mixtures, Halpin-Tsai models and Nielsen models are shown in Figures 13–15 for single filler formulations containing carbon black, synthetic graphite and carbon nanotubes in polypropylene, respectively. The rule of mixtures was not included in these figures, because it severely overpredicts the tensile modulus of the composites. The first observation we can make from this graphs, is that the inverse rule of mixtures model yielded the lowest values for the tensile modulus of the composites for all three fillers. In Figures 13 and 14, it can be observed that the Halpin-Tsai models are also underpredicting the tensile modulus of the composites with carbon black and synthetic graphite in polypropylene. However, Figure 15 is showing that the Halpin-Tsai models yield higher values when compared to the experimental data for composites with different amounts of carbon nanotubes. This result is likely due to the extremely high aspect ratio of carbon nanotubes.

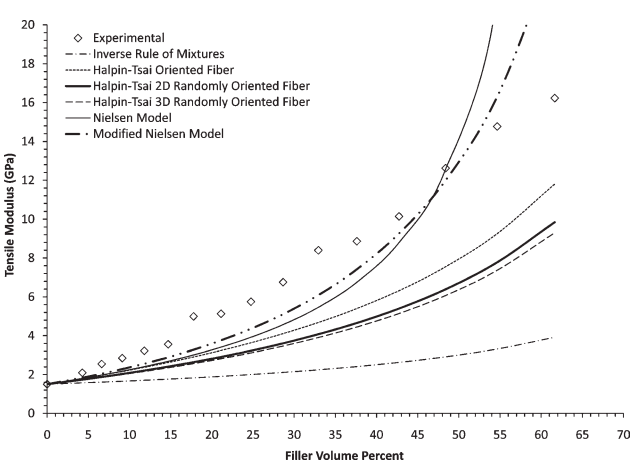

Figure 14 Tensile modulus modeling for synthetic graphite in polypropylene. From lowest to highest, the models at 55 wt% are Inverse Rule of Mixtures, 3D Halpin-Tsai, 2D Halpin-Tsai, Halpin-Tsai Oriented Fiber, Modified Nielsen, and Nielsen.

Nielsen's models

Nielsen's model uses the parameters A and ϕ_m, which depend on the shape and aspect ratio of fillers. These values are available in the literature[69,70] for different types of filler particles. The selected values are listed below:

Carbon black: $A = 1.5$ (spheres)

$\phi_m = 0.2$

Synthetic graphite: $A = 2(L/d)$ (uniaxially oriented rods with aspect ratio $L/d = 1.68$)

$\phi_m = 0.637$ (irregular particles)

Carbon nanotubes: $A = 8.38$ (random fibers with aspect ratio = 15, largest published value)

$\phi_m = 0.2$

It is noted that since the actual aspect ratio in our system is unknown, the A value of 8.38 for carbon nanotubes is only an estimate. Overall, the results given by the modified Nielsen's model [eq. (10)–(13)] appear to give reasonable results for SG/PP, CB/PP, and CNT/PP composites. This is consistent with that seen in the earlier study of Konell et al.[52] for carbon black and synthetic graphite fillers in

nylon 6,6 and in polycarbonate resins. However, Keith et al.[61] found that for composites containing synthetic graphite in Vectra, the Halpin-Tsai models performed the best, with the Nielsen model underpredicting the tensile modulus. This could be attributed to the poor adhesion of the synthetic graphite with the Vectra polymer.

CONCLUSIONS

Addition of different amounts of carbon fillers increases the tensile and flexural modulus of the composites. However, the ultimate tensile and flexural strengths for composites with carbon black and synthetic graphite as single fillers, decreased with higher filler concentrations. These results are consistent with that seen in the literature. Since carbon nanotubes have a much higher aspect ratio than CB and SG, the CNT/PP composites showed an increase in both the flexural and tensile ultimate strengths. The ultimate flexural strengths measured for all composites exceeded the 25 MPa requirement set by the Department of Energy for use of these materials in fuel cell bipolar plates applications.

Nanoscratch tests performed provide data that could be used to measure the degree of adhesion between fillers and the polymer matrix. The scratch results were represented by the normalized crest factor. When comparing crest factors of polypropylene composites with LCP composites, it can be seen that a better degree of adhesion exists for the carbon/polypropylene composites. Data analysis was done using the penetration into the composite surface as a function of the scratch distance and the results of this test agree with the results obtained for the tensile modulus of the composites. These results suggest that carbon-filled polypropylene composites may have suitability in fuel cell bipolar plate applications.

For this project, different tensile modulus models were applied, such as the rule of mixtures, inverse rule of mixtures, Halpin-Tsai oriented models and Nielsen models for composites containing different amount of carbon black, synthetic graphite and carbon nanotubes in polypropylene. The rule of mixtures and inverse rule of mixtures represent the high and low limits for the predicted values for the tensile modulus respectively. The Halpin-Tsai and the inverse rule of mixtures models underpredicted the tensile modulus of the composites containing carbon black and synthetic graphite. However, for formulations containing carbon nanotubes, the Halpin-Tsai overpredicts the tensile modulus values, due to the high aspect ratio of this filler. In all cases, the tensile modulus results obtained using modified Nielsen model showed better agreement with the experimental data. It can be observed that for the carbon black/polypropylene and synthetic graphite/polypropylene composites, there was a higher deviation if compared to the carbon nanotubes/polypropylene formulations.

The authors thank Asbury Carbons and Akzo Nobel for providing carbon fillers, American Leistritz technical staff for recommending an extruder screw design, Dow Chemical Company for providing the polypropylene polymer and Albert V. Tamashausky of Asbury Carbons for providing technical advice. The assistance of Stephen Macklin, Jeff Caspary, and Ben Harris undergraduate researchers was illustrious.

References

1. United States Department of Energy. "Technical Plan-Fuel Cells: Multi-Year Research, Development, and Demonstration Plan," Washington, DC, 3.4. Available at: www1.eere.energy.gov/hydrogenandfuelcells/mypp/pdfs/fuel_cells.pdf. Accessed March 2010.
2. Clulow, J. G.; Zappitelli, F. E.; Carlstrom, C. M.; Zemsky, J. L.; Busick, D. N.; Wilson, M. S. In Proceedings of the 2002 AIChE Spring National Meeting; New Orleans, LA, March 2002.
3. Bigg, D. M. Polym Eng Sci 1977, 17, 842.
4. Agari, Y.; Uno, T. J. J Appl Polym Sci 1985, 30, 2225.
5. Demain, A. Ph.D. Dissertation, Universite Catholique de Louvain, 1994.
6. Simon, R. M. Polym News 1985, 11, 102.
7. King, J. A.; Tucker, K. W.; Meyers, J. D.; Weber, E. H.; Clingerman, M. L.; Ambrosius, K. R. Polym Compos 2001, 22, 142.
8. Taipalus, R.; Harmia, T.; Zhang, M. Q.; Friedrich, K. Compos Sci Technol 2001, 61, 801.
9. Bao, S. P.; Tjong, S. C. Mater Sci Eng A 2008, 485, 508.
10. Wilson, M. S.; Busick, D. N. U.S. Pat. 6,248,467 (2001).
11. Loutfy, R. O.; Hecht, M. U.S. Pat. 6,511,766 (2003).
12. Braun, J. C.; Zabriskie, J. E.; Netzler, J. K.; Fuchs, M.; Gustafson, R. C. U.S. Pat. 6,180,275 (2001).
13. Mehta, V.; Cooper, J. S. J Power Sources 2003, 114, 32.
14. Petrovic, Z. S.; Martinovic, B.; Divjakovic, V.; Budinski-Simendic, J. J Appl Polym Sci 1993, 49, 1659.
15. Kaynak, A.; Polat, A.; Yilmazer, U. Mater Res Bull 1996, 31, 1195.
16. Chiu, H.-T.; Chiu, W.-M. J Appl Polym Sci 1996, 61, 607.
17. Narkis, M.; Lidor, G.; Vaxman, A.; Zuri, L. J Electrostatics 1999, 47, 201.
18. Chodak, I.; Omastova, M.; Pionteck, J. J Appl Polym Sci 2001, 82, 1993.
19. Gorga, R. E.; Cohen, R. E. J Polym Sci Part B: Polym Phys 2004, 42, 2690.
20. Liu, T.; Phang, I. Y.; Shen, L.; Chow, S. Y.; Zhang, W.-D. Macromolecules 2004, 37, 7214.
21. Arai, T.; Tominaga, Y.; Asai, S.; Sumita, M. J Polym Sci Part B: Polym Phys 2005, 43, 2568.
22. López Manchado, M. A.; Valentini, L.; Biagiotti, J.; Kenny, J. M. Carbon 2005, 43, 1499.
23. Fornes, T. D.; Baur, J. W.; Sabba, Y.; Thomas, E. L. Polymer 2006, 47, 1704.
24. Mali, T. M. A. S. Masters of Applied Science Thesis, University of Waterlee, Canada, 2006.
25. Zhou, Z.; Wang, S.; Zhang, Y. J Appl Polym Sci 2006, 102, 4823.
26. Kalaitzidou, K.; Fukushima, H.; Miyagawa, H.; Drzal, L. Polym Eng Sci 2007, 47, 1796.
27. Liu, T.; Tong, Y.; Zhang, W.-D. Compos Sci Technol 2007, 67, 406.
28. Akinci, A. Arch Mater Sci Eng 2009, 35, 91.

29. Ansari, M. N. M.; Ismail, H.; Zein, S. H. S. J Reinf Plast Compos 2009, 28, 2473.
30. Blunk, R. H.; Lisi, D.; Yoo, Y.-E.; Tucker, C. L. AIChE J 2003, 49, 18.
31. Mighri, F.; Huneault, M. A.; Champagne, M. F. Polym Eng Sci 2004, 44, 1755.
32. Cunningham, B. D.; Huang, J.; Baird, D. G. J Power Sources 2007, 165, 764.
33. Hauser, R. Ph.D. Dissertation, Michigan Technological University, 2008.
34. Barton Carter, R. L. Ph.D. Dissertation, Michigan Technological University, 2008.
35. King, J. A.; Keith, J. M.; Glenn, O. L.; Miskioglu, I.; Cole, A. J.; Mclaughlin, S. R.; Pagel, R. M. J Appl Polym Sci 2008, 108, 1657.
36. Keith, J. M.; King, J. A.; Grant, P. W.; Cole, A. J.; Klett, B. M.; Miskioglu, I. Polym Compos 2008, 29, 15.
37. King, J. A.; Johnson, B. A.; Via, M. D.; Ciarkowski, C. J. J Appl Polym Sci 2009, 112, 425.
38. King, J. A.; Johnson, B. A.; Via, M. D.; Ciarkowski, C. J. Polym Compos 2010, 31, 497.
39. Dow Chemical Company. The Dow Chemical Company Polypropylene Resin Product Literature, Form 167-00162-0905X; Dow Chemical Company: Midland, MI, 2005.
40. Akzo Nobel. Akzo Nobel Electrically Conductive Ketjenblack Product Literature; Akzo Nobel: Chicago, IL, 1999.
41. Asbury Carbons. Asbury Carbons Product Information; Asbury Carbons: Asbury, NJ, 2004.
42. Conoco. Conoco Carbons Products Literature; Conoco, Inc.: Houston, TX, 1999.
43. Hyperion Catalysis International. Hyperion Catalysis International Fibril Product Literature; Hyperion Catalysis International: Cambridge, MA, 2008.
44. King, J. A.; Morrison, F. A.; Keith, J. M.; Miller, M. G.; Smith, R. C.; Cruz, M.; Neuhalfen, A. M.; Barton, R. L. J Appl Polym Sci 2006, 101, 2680.
45. Standard Test Methods for Tensile Properties of Plastics, ASTM Standard D 638, American Society for Testing and Materials, Philadelphia, 1998.
46. Standard Test Methods for Flexural Properties of Unreinforced and Reinforced Plastics and Electrical Insulating Materials, ASTM Standard D 790-03, American Society for Testing and Materials, Philadelphia, 2004.
47. Broch, J. T. Mechanical Vibrations and Shock Measurements; Bruel and Kjaer: Naerum, Denmark, 1972.
48. Heiser, J. A.; King, J. A.; Konell, J. P.; Miskioglu, I.; Sutter, L. L. J Appl Polym Sci 2004, 91, 2881.
49. Konell, J. P.; King, J. A.; Miskioglu, I. Polym Compos 2004, 25, 172.
50. King, J. A.; Barton, R. L.; Hauser, R. A.; Keith, J. M. Polym Compos 2008, 29, 421.
51. King, J. A.; Miller, M. G.; Barton, R. L.; Keith, J. M.; Hauser, R. A.; Peterson, K. R.; Sutter, L. L. J Appl Polym Sci 2006, 99, 1552.
52. Konell, J. P.; King, J. A.; Miskioglu, I. J Appl Polym Sci 2003, 90, 1716.
53. Coleman, J. N.; Khan, U.; Guńko, Y. K. Adv Mater 2006, 18, 689.
54. Brcic, M.; Canadija, M.; Brnic, J.; Lanc, D.; Krscanski, S.; Vukelic, G. Est J Eng 2009, 15, 77.
55. Blake, R.; Guńko, Y. K.; Coleman, J.; Cadek, M.; Fonseca, A.; Nagy, J. B.; Blau, W. J. J Am Chem Soc 2004, 126, 10226.
56. Huang, J.-C. Adv Polym Technol 2002, 21, 299.
57. King, J. A.; Buttry, D. A.; Adams, D. F. Polym Compos 1993, 14, 292.
58. King, J. A.; Buttry, D. A.; Adams, D. F. Polym Compos 1993, 14, 301.
59. Ticona. "Vectra Liquid Crystal Polymer (LCP)." Available at: www.ticona.com/markets/vectrabr_e.pdf. Accessed March 2010.
60. Vallejo, F. J.; Iribarren, I.; Eguiazábal, J. I.; Nazábal, J. Polym Eng Sci 2002, 42, 1686.
61. Keith, J. M.; King, J. A.; Miskioglu, I.; Roache, S. C. Polym Compos 2009, 30, 1166.
62. King, J. A.; Miskioglu, I.; Wright-Charlesworth, D. D.; Van Karsen, C. D. J Appl Polym Sci 2007, 103, 328.
63. Agarwal, P. D.; Broutman, L. J. Analysis and Performance of Fiber Composites; Wiley: New York, 1980.
64. Mallick, P. K. Composites Engineering Handbook; Marcel Dekker: New York, 1997.
65. Halpin, J. C.; Kardos, J. L. Polym Eng Sci 1976, 16, 344.
66. Halpin, J. C. J Compos Mater 1969, 3, 732.
67. Nielsen, L. E. Ind Eng Chem Fundam 1974, 13, 17.
68. Bigg, D. M. Polym Compos 1986, 7, 125.
69. Nielsen, L. E.; Landel, R. F. Mechanical Properties of Polymers and Composites, 2nd ed.; Marcel Dekker: New York, 1994.
70. Nielsen, L. E. J Appl Phys 1970, 41, 4626.
71. McGee, S.; McCullough, R. L. Polym Compos 1981, 2, 149.
72. Li, C.; Chou, T.-W. Compos Sci Technol 2003, 63, 1517.
73. Kashyap, K. T.; Patil, R. G. Bull Mater Sci 2008, 31, 185.